Heliyon 9 (2023) e21400

Contents lists available at ScienceDirect

Heliyon

journal homepage: www.cell.com/heliyon

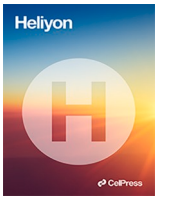

Targeted delivery of oxaliplatin via folate-decorated niosomal nanoparticles potentiates resistance reversion of colon cancer cells

Siham Abdulzehra [a,1], Davoud Jafari-Gharabaghlou [a,1], Nosratollah Zarghami [a,b,*]

[a] Department of Clinical Biochemistry and Laboratory Medicine, Faculty of Medicine, Tabriz, University of Medical Sciences, Tabriz, Iran
[b] Department of Medical Biochemistry, Faculty of Medicine, Istanbul Aydin University, Istanbul, Turkey

ARTICLE INFO

Keywords:
Oxaliplatin
Colorectal cancer
Drug resistance
Niosomal nanoparticles
Targeted delivery

ABSTRACT

Background: Colorectal cancer (CRC) is a prevalent type of cancer, ranking third in incidence and fourth in cancer-related deaths globally. The increase in mortality rates related to colorectal cancer among younger patients is a cause for concern. Chemotherapy is the primary approach for palliative care in colon cancer, but the development of drug resistance limits its effectiveness. Apoptosis is a process of programmed cell death that plays a crucial role in regulating normal cell death and abnormal tissue degeneration in cancer. Genes such as caspase-3, caspase-9, p53, and survivin are involved in apoptosis induction. The field of nanotechnology has presented exciting opportunities for controlled drug delivery and addressing drug resistance in cancer. Niosomes are among the nanocarriers known for their impressive features, making them excellent candidates for drug delivery. In the current study, we investigate whether niosomal nanoparticles coated with FA have the ability to deliver oxaliplatin to drug-resistant cells effectively and potentially resistance reversion in colon cancer cells.

Methods: The niosomal nanoparticles (NPs) were fabricated using the thin-film hydration method and characterized using DLS (Dynamic Light Scattering), FTIR (Fourier Transform Infrared Spectroscopy), SEM (Scanning Electron Microscopy), and AFM (Atomic Force Microscopy) systems. The drug release and drug encapsulation efficiency of the NPs were also determined. An MTT assay was performed on oxaliplatin-resistant cells to determine the IC50 values of the drug in its pure and nano-encapsulated forms. Gene expression of caspase-3, caspase-9, p53, and survivin was investigated using the qRT-PCR (quantitative Reverse Transcription Polymerase Chain Reaction) technique, and cell apoptosis or necrosis was quantified using flow cytometry.

Results: Size, PDI, zeta potential, morphology, drug release, and encapsulation efficiency of fabricated niosomal NPs were acceptable. Oxaliplatin anti-cancer drug showed a higher impact on cancerous cells in nano-encapsulated form. The expression level of caspase-3, caspase-9, and p53 was increased which was in confirmation by flow cytometry results.

Conclusion: Taken together, results of this study demonstrated potential effect of folate decorated oxaliplatin-loaded niosomal NPs to resistance-reversion of Oxaliplatin-resistance colon cancer cells.

* Corresponding author. Clinical Biochemistry and Laboratory Medicine Faculty of Medicine of Medical Sciences Tabriz, Iran.
E-mail address: zarghami@tbzmed.ac.ir (N. Zarghami).
[1] Co-first Authors (these authors contributed equally to this work).

https://doi.org/10.1016/j.heliyon.2023.e21400
Received 8 September 2023; Received in revised form 8 October 2023; Accepted 20 October 2023
Available online 29 October 2023

1. Introduction

Colorectal cancer (CRC) ranks as the third most common type of cancer and is the fourth leading cause of cancer-related deaths, with approximately 700,000 fatalities annually [1]. Additionally, there has been a noticeable rise in mortality rates related to CRC among younger patients over the past ten years [2]. CRC is commonly treated with chemotherapy as the primary approach for palliative care. The treatment typically involves the use of fluoropyrimidines like 5-fluorouracil, either alone or in combination with leucovorin, and other cytotoxic agents like oxaliplatin or irinotecan. The addition of leucovorin is often recommended to minimize treatment-related toxicity, and the incorporation of other cytotoxic agents has demonstrated the potential to enhance response rates and prolong progression-free survival. These drugs often cause adverse side effects [1]. The effectiveness of chemotherapies utilized in the treatment of cancer is limited by a significant issue known as drug resistance. Before undergoing treatment, tumors may already possess intrinsic resistance to chemotherapy, making them apoptosis-resistance [3]. Apoptosis is the process of programmed cell death that is activated in cells that have experienced irreparable damage or undergone mutations and may contribute to cancer formation [4]. Several genes including caspase-3, caspase-9, survivin, and p53 are involved in apoptosis induction [5–7]. Apoptosis basically relies on caspases as mediators. One of the most commonly activated death proteases in this process is caspase-3, which plays a critical role in catalyzing the targeted cleavage of numerous important proteins within the cell [5,8–10]. Caspase-9 is recognized for its rule in starting intrinsic apoptosis. It plays a crucial role in regulating both normal programmed cell death and abnormal tissue degeneration [6]. Survivin belongs to a group of proteins called inhibitors of apoptosis protein family, which has the ability to prevent caspases and hinder cell death. It is overexpressed in the majority of cancers and linked with unfavorable clinical prognosis [7,11–13]. While a lot of cancers are initially vulnerable to chemotherapy, they may gradually acquire resistance through several mechanisms such as DNA damage repair, drug target alteration, drug efflux, epithelial-mesenchymal transition, drug inactivation, and cell death inhibition [14]. Acquired resistance is a vexing characteristic as it not only makes tumors resistant to the drugs that were initially employed to treat them but can also lead to cross-resistance to other drugs that work through diverse mechanisms. Intrinsic or acquired drug resistance is thought to be responsible for treatment failure in more than 90 % of individuals diagnosed with metastatic cancer, and micrometastatic tumor cells that have developed resistance may also impair the efficacy of chemotherapy in the adjuvant context. Accordingly, overcoming drug resistance would result in a considerably significant improvement in survival rates [3]. The nanotechnology field has presented for controlled drug delivery and addressing drug resistance in cancer. In particular, nanoparticles ranging from 10 to 200 nm in diameter have exhibited more favorable pharmacokinetic profiles than small-molecule drugs. These drug-loaded nanoparticles demonstrate superior tumor accumulations, sustained drug release, and prolonged systemic circulation period via both active and passive mechanisms [15,16]. Several nanoparticle platforms, such as mesoporous silica particles, polymeric micelles, liposomes, dendrimers, and niosome have been employed to transport various classes of therapeutics, including chemosensitizers, small interference RNA, antiangiogenic agents, and cytotoxic agents [15,17,18]. Niosomes are novel drug delivery systems consisting of bilayer vesicles that enable sustained, controlled, and targeted administration of drugs [19–22]. For example, Ashkezari et al., used a highly biocompatible nanocarrier based on niosomal formulation to show the combination therapy of inorganic nanoparticles and sultamicillin antibiotic on bacterial growth inhibition [23]. In another study a 3D-printed gelatin-alginate scaffolds containing paclitaxel-loaded niosomes used in against breast cancer cells (MCF-7), anticancer effect of the designed nanocarrier showed a significant increase in the expression and activity of apoptosis promoting genes and a remarkable decrease in metastasis-enhancing genes [24]. Zaer et al., used a 3D-printed gelatin-alginate nanocomposites containing doxorubicin-loaded niosomes (Nio-DOX@GT-AL) against MCF-7 breast cancer cells that result in decreasion of necrosis and enhance of apoptosis in these cells [25]. Compared to other nano drug delivery systems, niosomes offer numerous advantages, such as their ability to simultaneously deliver both hydrophobic and hydrophilic substances, their non-toxic nature due to the use of non-ionic surfactants, and their sustained drug release at a low cost. Additionally, the functional group present on the hydrophilic head allows for easy formation and modification of the surface of niosomes [19,20]. For example, Honarvari et al., fabricated niosomal nanoparticles (NPs) decorated with polyethylene glycol (PEG) and folic acid (FA) to target breast cancer cells [26]. Many cancer cells exhibit upregulated folate receptors, while their expression level is typically low in normal cells. This disparity allows for the selective targeting of cancer cells through the conjugation of FA to nanostructures, which selectively bind to cancer cells that overexpress folate receptors [27,28]. The aim of this research was to explore the effectiveness of niosomal NPs coated with FA in delivering oxaliplatin to cancer cells that had become resistant to the drug. The focus was on examining whether this drug delivery system could trigger apoptosis.

2. Material and methods

2.1. Synthesis of folic acid decorated niosomal NPs

To synthesize blank niosomal NPs decorated with folic acid (Fol-Nio), a mixture of ethanol (5 ml) and chloroform (5 ml) was used to dissolve cholesterol (6 mg), and span 60 (36 mg). The resulting solution was evaporated using a rotary evaporator at 60 °C temperature and 120 rpm under reduced pressure, leading to the formation of a thin film at the bottom of the round bottom flask. The resulting Fol-Nio was fabricated by adding 2.2 mg of folic acid and hydrating the thin film with 10 ml of PBS at 55 °C, followed by drying the reactants at 55 °C and 150 rpm for 60 min. The obtained solvent was collected and sonicated for 30 min using a sonicator to produce uniform, smaller, and more homogenized niosomal NPs. To fabricate folate-coated niosomal nanoparticles containing oxaliplatin (Fol-Nio/Oxp), the identical protocol was employed, with the only alteration being the incorporation of 3.97 mg of oxaliplatin into the PBS during the hydration phase. For the creation of blank niosomal nanoparticles (Nio) and oxaliplatin-loaded niosomal nanoparticles (Nio/Oxp), identical procedures and quantities were employed, except that the synthesis process did not involve the use of folic acid

[26,29].

2.2. Characterization of niosomal NPs

AFM (JPK Instruments AG, Berlin, Germany) and SEM (MIRA3 TESCAN, Czech) systems were utilized to study the morphology, aggregation, size, and dispersion of synthesized NPs. Fourier-transform infrared spectroscopy (Shimadzu 8400 S, Kyoto, Japan) was used to analyze the physicochemical structures of FA, oxaliplatin, and synthesized NPs. Finally, the zeta potential, particle size, and dispersion index (PDI) of NPs were evaluated with a dynamic light scattering (DLS) system (Nano ZS, Malvern Instruments Ltd., Malvern, UK) [30,31].

2.3. Release pattern of oxaliplatin

10 mL of Fol-Nio/Oxp NPs and Nio/Oxp NPs were placed in separate dialysis bags with a molecular weight cutoff (MWCO) of 12 kDa and the following processes were performed for both to determine oxaliplatin release from each NPs. The mixture was stirred using a magnetic stirrer at a speed of 150 rpm for 140 h at a temperature of 37 °C under 4.4 (cancerous) pH and 7.4 (normal physiological) pH conditions. At predetermined intervals, a specific amount of release medium was withdrawn and replaced with the same amount of fresh PBS. The exuded oxaliplatin was assessed using an ultraviolet-light spectrophotometer (PerkinElmer, Fremont, CA, USA) at λmax of oxaliplatin (510 nm). An equal concentration of oxaliplatin was used as a control in this test [32,33].

2.4. Entrapment efficiency of oxaliplatin

In order to measure the amount of oxaliplatin in the NPs, the supernatant was separated following the production of Fol-Nio/Oxp NPs and Nio/Oxp NPs using membrane dialysis in PBS at 4 °C. The determination of pure oxaliplatin in the aqueous phase was performed using an ultraviolet spectrophotometer (PerkinElmer, Fremont, CA, USA) at wavelength 510 nm. To calculate the percentage of oxaliplatin encapsulated in the niosomal NPs (EE), the following formulas were employed [33,34]:

$$\text{Entrapment Efficiency of Fol} - \text{Nio} \Big/ \text{Oxp} = \frac{\text{Oxaliplatin in Fol-Nio/Oxp NPs}}{\text{Initial oxaliplatin}} \times 100\%$$

$$\text{Entrapment Efficiency of Nio} \Big/ \text{Oxp} = \frac{\text{Oxaliplatin in Nio/Oxp NPs}}{\text{Initial oxaliplatin}} \times 100\%$$

2.5. Drug resistant colon cancer cells

The oxaliplatin-resistant SW480 cells were obtained from oxaliplatin-sensitive SW480 cells as described in the previous study [35]. Both cell lines were grown in RPMI-1640 medium (Sigma, Germany) enriched with 10 U/mL of penicillin (Sigma, Germany), 10 % fetal bovine serum (Biochrom, UK), and 10 μg/ml of streptomycin (Sigma, Germany) to promote cell growth and survival. The cells were cultivated at a temperature of 37 °C with 5 % CO_2 to maintain optimal physiological conditions for their growth [36].

2.6. In vitro cytotoxicity assay

The cytotoxicity test of pure oxaliplatin, Fol-Nio/Oxp NPs, Nio/Oxp NPs, Fol-Nio NPs, and blank niosomal NPs on oxaliplatin-resistant and oxaliplatin-sensitive cells was performed by MTT assay. Briefly, 10^4 oxaliplatin-resistant SW480 cells and 10^4 oxaliplatin-sensitive SW480 were separately seeded in each well of a 96-well plate for 24 h. Cells were treated with different concentrations of pure oxaliplatin, Fol-Nio/Oxp NPs, Nio/Oxp NPs, Fol-Nio NPs, and blank niosomal NPs. The consumed amount of each substance is given in Table 1. After 48 h the medium containing the drug was removed from the plate and 200 μL of MTT (Sigma, Germany) solution was injected into each well forwarded with incubation for 4 h at 37 °C. 100 μL of DMSO (Merck, Germany) was added to each well and the 96-well plate was shaken for 15 min. Finally, the Absorbance of each well was measured using an EL × 800 Microplate Absorbance Reader (Bio-Tek Instruments) at 570 nm and IC50 of pure oxaliplatin, oxaliplatin-loaded niosomal NPs, and

Table 1
The quantities of pure oxaliplatin, Fol-Nio/Oxp NPs, Nio/Oxp NPs utilized for the MTT test on oxaliplatin-resistant SW480 cells and oxaliplatin-sensitive SW480 (All concentrations are in micromolar).

oxaliplatin-resistant SW480			oxaliplatin-sensitive SW480		
Pure oxaliplatin	Fol-Nio/Oxp NPs	Nio/Oxp NPs	Pure oxaliplatin	Fol-Nio/Oxp NPs	Nio/Oxp NPs
1	1	1	0.1	0.1	0.1
5	5	5	0.5	0.5	0.5
10	10	10	1	1	1
20	20	20	2	2	2
30	30	30	4	4	4
40	40	40	6	6	6

blank niosomal NPs were calculated by Graph Pad Prism software [22,37].

2.7. Gene expression analyses

Oxaliplatin-resistant cells were treated with pure oxaliplatin, Fol-Nio/Oxp NPs, Nio/Oxp NPs, for 48 h. Subsequently, the cells were washed with PBS and subjected to vortexing with the addition of 50 L of PBS. To fix the samples, 1 mL of cold 70 % ethanol was added to cells while shaking the cells to prevent clumping. Next, the fixed cells were refrigerated for 2 h, followed by centrifugation and a single wash with PBS. The cells were then exposed to 1 mL of master mix solution and 1 mL of PBS containing 0.1 % (v/v) Triton X-100. To produce complementary DNA (cDNA), the extracted RNA was combined with 10 μL of reaction buffer (2 ×), 5 g of RNA, and 2 μL of Enzyme-Mix in RNase-free tubes containing 20 L of DEPC-treated water. The mixture was incubated at 25 °C for 10 min followed by 60 min at 47 °C before analysis. Subsequently, in order to inactivate of RT enzyme, the samples were incubated at 85 °C for 5 min. To examine the expression levels of caspase-3, caspase-9, p53, survivin, and GAPDH, a Bio-Rad IQ5 Real-Time PCR instrument (Hercules, CA, USA) was used along with SYBR Master Mix (Life Technologies Applied Biosystems, UK). Table 2 contains the forward and reverse primer sequences for each of these genes [37].

2.8. Apoptosis

A flow cytometry technique was utilized to determine the proportion of oxaliplatin-resistant cells undergoing apoptosis. The cells were treated with pure oxaliplatin, Fol-Nio/Oxp NPs, Nio/Oxp NPs for 48 h, and then labeled with fluorescent dyes using the Apoptosis and Necrosis Quantitation Kit to distinguish between apoptotic and necrotic cells. After being resuspended in 1X binding buffer and washed twice with PBS, the cells were stained with propidium iodide (red fluorescence) and annexin V-FITC (green fluorescence) and analyzed using a benchtop flow cytometer (FACSCalibur, BD Biosciences, USA) [26].

3. Results and discussion

Vesicular drug delivery systems comprising of a bilayer membrane and a hollow space have earned significant interest as potential drug delivery. These systems exhibit high entrapment efficiency, storage time varying from low to high, a receptive surface that can be utilized to treat various targeting agents, the ability to be synthesized by smart components for targeting specific environments, and the capability of delivering both hydrophobic and hydrophilic drugs [38]. Niosomes are microscopic bilayer structures that are formed by the self-association of hydrated surfactant monomers. These structures have a non-ionic surfactant vesicle composition and come in sizes ranging from 10 to 1000 nm [39]. Fig. 1 shows the size of synthesized Fol-Nio/Oxp NPs by DLS analysis. As expected, the average size of oxaliplatin-loaded niosomal NPs is larger than blank niosomal NPs, which is due to the entrapment of the oxaliplatin drug among the synthesized niosomes.

The stability of a colloid system can be determined by measuring its zeta potential, which is a crucial criterion [40]. The zeta potential of blank niosomal NPs and Nio/Oxp NPs evaluated to be -11.67 ± 5.1 and -26.54 ± 3.2 respectively. Table 3 lists properties measurement for the rest of niosomal NPs by DLS.

The shape and structure of nanoparticles have been demonstrated to have a significant impact on various characteristics, including how long they circulate in the body, how they interact with cells, and their flow dynamics [41]. The morphology of synthesized niosomal NPs was studied by AFM and SEM microscopic systems (Fig. 2).

FTIR spectroscopy was used to identify niosomal NPs, oxaliplatin, and folic acid (Fig. 3). At around 573 cm^{-1}, oxaliplatin displays a pinnacle that matches the Pt–N stretching vibrations and also emits a signal of symmetric Pt–O stretching at approximately 808 cm^{-1}. Also, peaks at 3507.67 cm^{-1} (–NH) and at 1711.88 cm^{-1} (C═O) are recognized. Folic acid is clearly defined with C═O stretching at 1651 cm^{-1}. The FTIR analysis of the niosomal nanoparticles indicates a significant peak within the 3000-3700 cm^{-1} range, which is indicative of a robust hydrogen bond resulting from the combination of materials. Previous research suggests that this bond is primarily formed between cholesterol and span 60 [42].

A study on the release of oxaliplatin from Fol-Nio/Oxp NPs and Nio/Oxp NPs was conducted under both cancerous and physiological pH conditions (4.4 and 7.4). The results of the 140-h release profile in PBS at 37 °C are presented in Fig. 4. The study revealed that after 140 h at pH 4.4, 88 % and 62 % of the loaded oxaliplatin were released from the Nio/Oxp NPs and Fol-Nio/Oxp NPs, respectively. Whereas, 45 % and 34 % of the loaded oxaliplatin were released from the Nio/Oxp NPs and Fol-Nio/Oxp NPs, respectively at pH 7.4 at the same time interval. These results indicate that drug release of niosomal NPs is pH dependent and within the same condition, a higher amount of drug releases. The cumulative release profile of oxaliplatin exhibited a biphasic pattern wherein the

Table 2
Primer sequences list used for qRT-PCR.

Genes	Forward (5′ → 3′)	Reverse (5′ → 3′)
p53	CCCACTTCACCGTACTAACCAG	CATTTCACAGATATGGGCCTT
Survivin	GCCTCTGTACTCATCTAAGCTG	ACAAAGCCAATTACTAAGCAAC
Caspase-3	CCTTCCATCAAATAGAACCAC	ATTGCCTCTCATAATGACTGC
Caspase-9	GTTCTCAGACCGGAAACACC	CAGGATGTAAGCCAAATCTGC
GAPDH	ATATTGTTGCCATCAATGACCC	TTCCCGTTCTCAGCCTTGACG

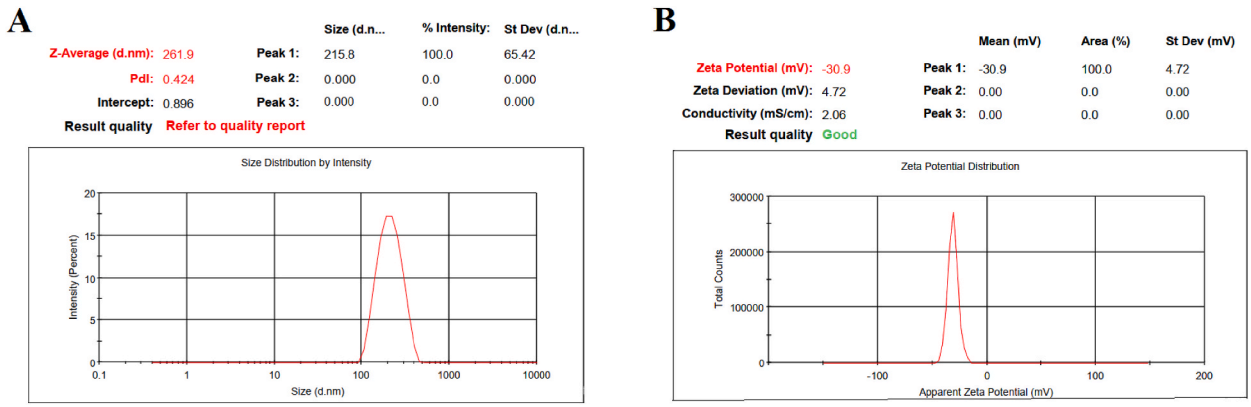

Fig. 1. Average size, zeta potential, and PDI of synthesized Fol-Nio/Oxp NPs.

Table 3
DLS characterizations of Blank niosomal NPs, Nio/Oxp NPs, and Fol-Nio/Oxp NPs.

Groups	Size (nm)	Polydispersity Index	Zeta-Potential (mV)
Blank niosomal NPs	149.2 ± 3.7	0.616	−11.67 ± 5.1
Nio/Oxp NPs	193 ± 7.4	0.587	−26.54 ± 3.2
Fol-Nio/Oxp NPs	215 ± 6.2	0.424	−30.9 ± 4.72

maximum release rate was observed during the first 24 h of the experiment (at 47 % and 81 % for Nio/Oxp NPs and Fol-Nio/Oxp NPs, respectively) and decreased thereafter. It was found that the initial release of oxaliplatin occurred due to its weak bonding with the surface of niosomal NPs, instead of being loaded inside the NPs. In term of stability niosomal NPs have demonstrated exceptional properties. For instance, Shahbazi et al. reported an approximately 19.14 % increase in the size of the FA NPs after two months of storage at 25 ± 1 °C [43].

The study on drug encapsulation efficiency indicated that the oxaliplatin-loaded niosomal nanoparticles had an entrapment efficiency of 83.6 %.

The growth of oxaliplatin-resistant SW480 cells was significantly inhibited in a dose-dependent manner by pure oxaliplatin, Nio/Oxp NPs, and Fol-Nio/Oxp NPs as demonstrated in Fig. 5. IC50 values for pure oxaliplatin Nio/Oxp NPs, and Fol-Nio/Oxp NPs are presented in Table 4. It was found that Nio/Oxp NPs and Fol-Nio/Oxp NPs were more effective than pure oxaliplatin when administered at the same concentration due to their increased solubility in the aqueous medium, facilitated passage through the cell membrane, and higher bioavailability. The blank niosome and Fol-Nio NPs did not have a significant impact on any of the cell types even at high doses. As per the results of the MTT assay, the treatment group receiving blank niosomes and Fol-Nio NPs was excluded from subsequent tests, and the remaining experiments in the study were performed using IC50 values of pure oxaliplatin, Nio/Oxp NPs, and Fol-Nio/Oxp NPs as treatment groups.

To assay, whether treatments affect the expression of the studied genes, the cells were treated with drugs for 48 h then RT-PCR was done (Fig. 6). The result showed a significant increase in the expression of caspase-3, caspase-9, and p53 in the oxaliplatin-resistant cells and a decrease in survivin gene. Apoptosis, the process of programmed cell death, relies heavily on the activity of caspase 3, a vital enzyme. Once activated, caspase 3 breaks down different substrates found within the cell, causing distinct morphological and biochemical alterations linked to apoptosis. As a result, caspase 3 activity usually rises during apoptosis. Caspase 9 is also an important enzyme involved in apoptosis. It is a member of the caspase family of cysteine proteases and is considered to be an initiator caspase, which means it plays a key role in triggering the apoptotic pathway. In response to certain signals such as DNA damage or cellular stress, caspase 9 is activated and subsequently cleaves and activates downstream effector caspases such as caspase 3, leading to apoptosis. p53 is a tumor suppressor protein that plays a key role in regulating cell division and preventing the development of cancer. In response to various cellular stresses such as DNA damage, p53 is activated and can induce cell cycle arrest or initiate apoptosis depending on the severity of the damage. The protein Survivin belongs to the inhibitor of apoptosis (IAP) family and primarily functions to promote cell survival by preventing apoptosis. It works by binding to caspases, inhibiting their activity and thus halting apoptosis. Although survivin is typically present during embryonic development and rapid cell division, its expression levels are often reduced in normal adult tissues. In contrast, in many cancer types, survivin is highly expressed which can lead to tumor growth and resistance to chemotherapy-induced apoptosis. The study revealed that treatment with Nio/Oxp NPs and Fol-Nio/Oxp NPs exhibited significant downregulation of survivin, while upregulation of caspase-3, caspase-9 and, p53 in the resistant cells than the pure oxaliplatin which, as previously mentioned, is due to the increased bioavailability of oxaliplatin by niosomal nanoparticles.

In order to further investigate the induction of apoptosis on oxaliplatin-resistant by the oxaliplatin in pure and nano form a flow cytometry was used (Fig. 7). As in the previous tests, oxaliplatin-loaded niosomal NPs have a greater effect at the same dose compared to the pure oxaliplatin on drug-resistant cells. The control group shows the highest number of viable cells as no drugs were used as

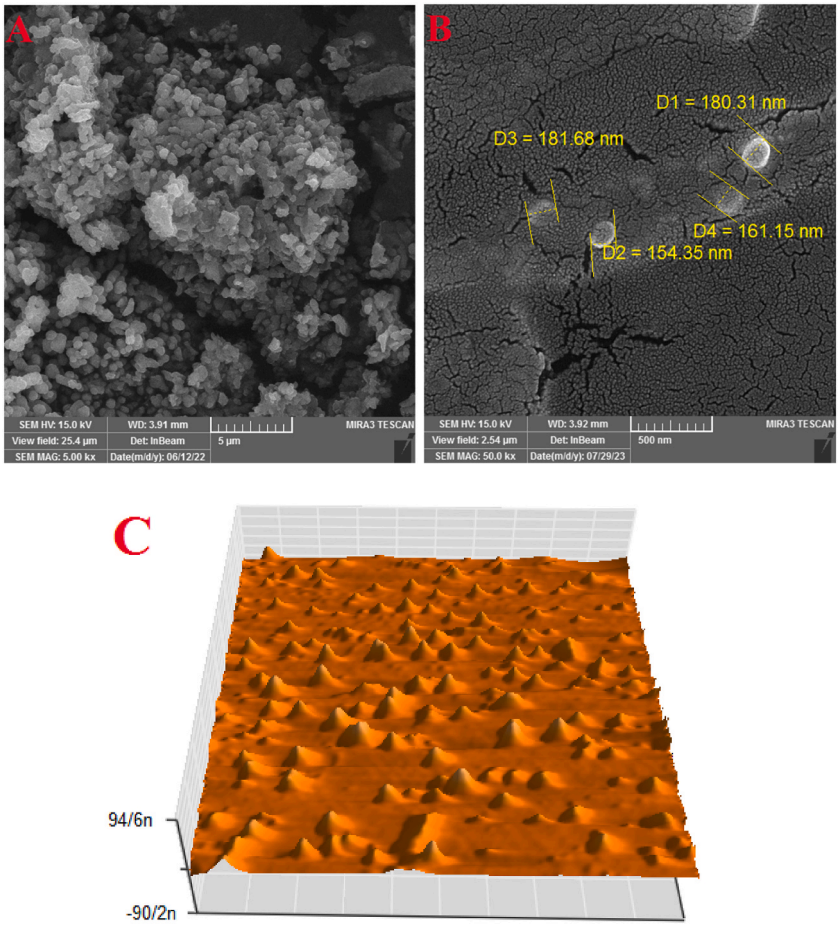

Fig. 2. SEM (A, B) and AFM (C) images of synthesized Fol-Nio/Oxp NPs.

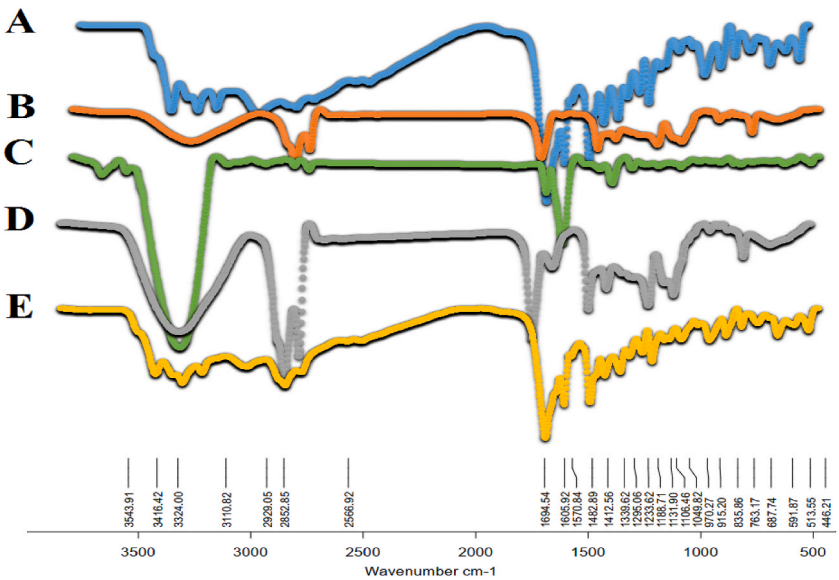

Fig. 3. FTIR results of (A) folate, (B) blank nisome, (C) oxaliplatin, (D) Nio/Oxp NPs, and (E) Fol-Nio/Oxp NPs.

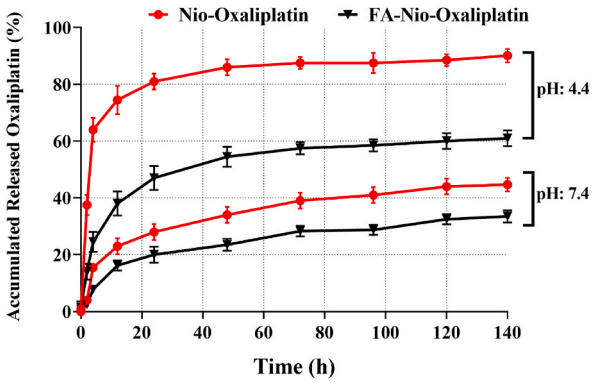

Fig. 4. 140 h in-vitro release pattern of oxaliplatin from niosomal NPs. The pores of the dialysis membrane used in the experiment were adequately large to enable unrestricted movement of oxaliplatin, while also being small enough to prevent the diffusion of nanoparticles.

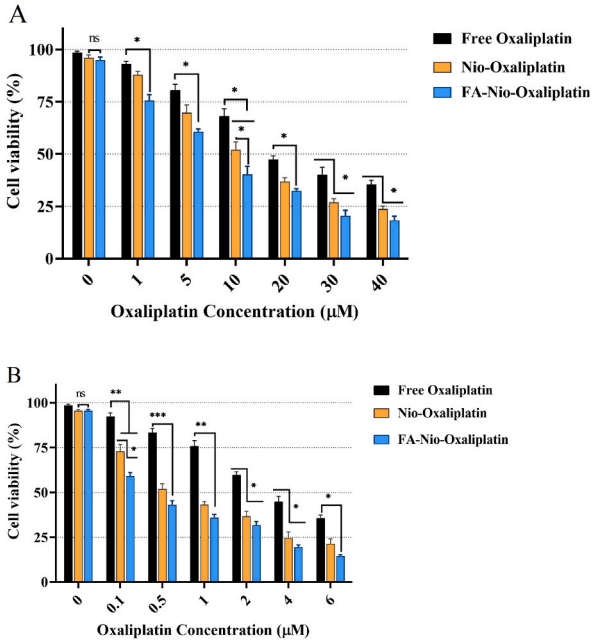

Fig. 5. MTT assay result of oxaliplatin-resistant and oxaliplatin-sensitive cells treated with oxaliplatin, Fol-Nio/Oxp NPs, and Nio/Oxp NPs. A) oxaliplatin-resistant SW480 cells, B) oxaliplatin-sensitive SW480 cells. The results of the assay demonstrated a gradual reduction in viable cells with the simultaneous rise in drug concentration.

Table 4
IC50 values of pure oxaliplatin, Nio/Oxp NPs, and Fol-Nio/Oxp NPs for oxaliplatin-resistant and oxaliplatin-sensitive cells.

Groups	Pure Oxaliplatin	Nio/Oxp NPs	Fol-Nio/Oxp NPs
Sensitive SW480	2.86 μM	0.53 μM	0.26 μM
Resistance SW480	19.24 μM	10.63 μM	7.21 μM

treatment. The lowest rate of early apoptosis occurred in cells treated with Fol-Nio/Oxp NPs, and this treatment group also had the highest rate of late apoptosis. Also, all the results of the apoptosis test are correlated with the results of the expression of genes involved in apoptosis, and more expression of apoptosis-inducing genes causes more apoptosis percentage.

4. Conclusion

The use of oxaliplatin in cancer treatment has been limited by the development of drug resistance. This study investigated the

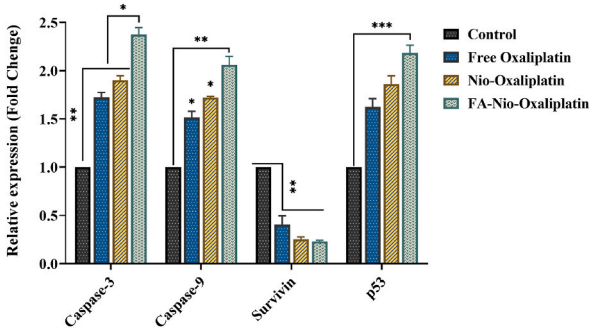

Fig. 6. Alterations in gene expression related to apoptosis (p value < 0.001 ***, p value < 0.01 **, and p value < 0.1 *).

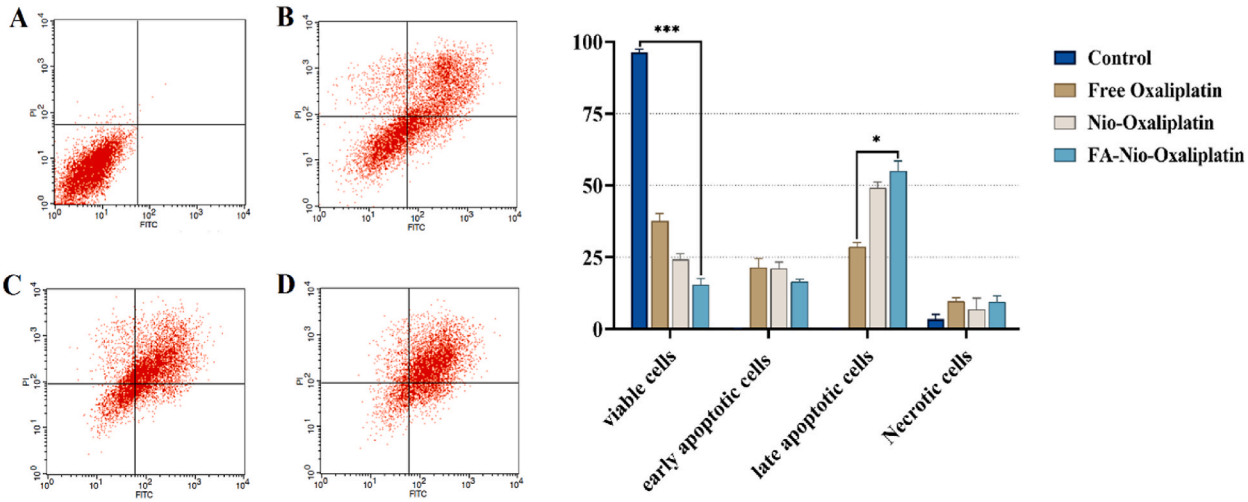

Fig. 7. The flow cytometric and Annexin V/PI staining assay results for the detection of apoptosis. A) Control, B) Free oxaliplatin, C) Nio/Oxp NPs, D) Fol-Nio/Oxp NPs (p value < 0.001 ***, and p value < 0.1 *).

efficacy of niosomal delivery of oxaliplatin in oxaliplatin-resistant cells. Our results showed that the niosomal delivery of oxaliplatin resulted in higher toxicity, increased apoptosis, decreased expression of drug resistance-related genes, and eventually resistance-reversion of drug-resistance colon cancer cells compared to conventional oxaliplatin treatment. Furthermore, the designed niosomal carriers were found to be acceptable in terms of size, polydispersity index (PDI), zeta potential, drug loading efficiency, and drug release. These findings suggest that niosomal delivery of oxaliplatin may be a promising strategy for overcoming drug resistance in cancer treatment. Further studies are needed to evaluate the safety and efficacy of this approach in clinical settings.

Availability of data and materials

The data and materials that support the findings of this study are available from the corresponding author, upon reasonable request.

Ethical approval

Not applicable.

Funding

The authors declare that no funds were received during the preparation of this manuscript.

CRediT authorship contribution statement

Siham Abdulzehra: Investigation, Methodology, Writing – original draft. **Davoud Jafari-Gharabaghlou:** Data curation, Formal analysis, Project administration, Software, Writing – review & editing. **Nosratollah Zarghami:** Conceptualization, Writing – review &

editing.

Declaration of competing interest

The authors declare that they have no known competing financial interests or personal relationships that could have appeared to influence the work reported in this paper.

References

[1] I. Mármol, et al., Colorectal carcinoma: a general overview and future perspectives in colorectal cancer, Int. J. Mol. Sci. 18 (1) (2017) 197.
[2] F.A. Sinicrope, Increasing incidence of early-onset colorectal cancer, N. Engl. J. Med. 386 (16) (2022) 1547–1558.
[3] D. Longley, P. Johnston, Molecular mechanisms of drug resistance, J. Pathol.: A Journal of the Pathological Society of Great Britain and Ireland 205 (2) (2005) 275–292.
[4] S. Elmore, Apoptosis: a review of programmed cell death, Toxicol. Pathol. 35 (4) (2007) 495–516.
[5] A.G. Porter, R.U. Jänicke, Emerging roles of caspase-3 in apoptosis, Cell Death Differ. 6 (2) (1999) 99–104.
[6] M.I. Avrutsky, C.M. Troy, Caspase-9: a multimodal therapeutic target with diverse cellular expression in human disease, Front. Pharmacol. 12 (2021), 701301.
[7] P.K. Jaiswal, A. Goel, R. Mittal, Survivin: a molecular biomarker in cancer, The Indian journal of medical research 141 (4) (2015) 389.
[8] Y. Alagheband, et al., Design and fabrication of a dual-drug loaded nano-platform for synergistic anticancer and cytotoxicity effects on the expression of leptin in lung cancer treatment, J. Drug Deliv. Sci. Technol. 73 (2022), 103389.
[9] S. Talaei, et al., Spotlight on 17-AAG as an Hsp90 inhibitor for molecular targeted cancer treatment, Chem. Biol. Drug Des. 93 (5) (2019) 760–786.
[10] A. Alibakhshi, et al., An update on phytochemicals in molecular target therapy of cancer: potential inhibitory effect on telomerase activity, Curr. Med. Chem. 23 (22) (2016) 2380–2393.
[11] N. Hassani, et al., The effect of dual bioactive compounds artemisinin and metformin co-loaded in PLGA-PEG nano-particles on breast cancer cell lines: potential apoptotic and anti-proliferative action, Appl. Biochem. Biotechnol. 194 (10) (2022) 4930–4945.
[12] Z. Davoudi, et al., Molecular target therapy of AKT and NF-kB signaling pathways and multidrug resistance by specific cell penetrating inhibitor peptides in HL-60 cells, Asian Pac. J. Cancer Prev. APJCP 15 (10) (2014) 4353–4358.
[13] S. Ghasemali, et al., Inhibitory effects of β-cyclodextrin-helenalin complexes on H-TERT gene expression in the T47D breast cancer cell line-results of real time quantitative PCR, Asian Pac. J. Cancer Prev. APJCP 14 (11) (2013) 6949–6953.
[14] G. Housman, et al., Drug resistance in cancer: an overview, Cancers 6 (3) (2014) 1769–1792.
[15] C.-M.J. Hu, L. Zhang, Nanoparticle-based combination therapy toward overcoming drug resistance in cancer, Biochem. Pharmacol. 83 (8) (2012) 1104–1111.
[16] K. Nejati, et al., Nanoparticle-based drug delivery systems to overcome gastric cancer drug resistance, J. Drug Deliv. Sci. Technol. 70 (2022), 103231.
[17] M.F.S. Jadid, et al., Enhanced anti-cancer effect of curcumin loaded-niosomal nanoparticles in combination with heat-killed Saccharomyces cerevisiae against human colon cancer cells, J. Drug Deliv. Sci. Technol. (2023), 104167.
[18] M. Dadashpour, et al., Increased pro-apoptotic and anti-proliferative activities of simvastatin encapsulated PCL-PEG nanoparticles on human breast cancer adenocarcinoma cells, J. Cluster Sci. 34 (1) (2023) 211–222.
[19] P. Bhardwaj, et al., Niosomes: a review on niosomal research in the last decade, J. Drug Deliv. Sci. Technol. 56 (2020), 101581.
[20] Z. Keshtmand, et al., Enhanced anticancer effect of Artemisia turcomanica extract in niosomal formation on breast cancer cells: in-vitro study, Nano-Structures & Nano-Objects 35 (2023), 101030.
[21] G. Shafiei, et al., Targeted delivery of silibinin via magnetic niosomal nanoparticles: potential application in treatment of colon cancer cells, Front. Pharmacol. 14 (2023).
[22] F. Ghorbanzadeh, et al., Advanced nano-therapeutic delivery of metformin: potential anti-cancer effect against human colon cancer cells through inhibition of GPR75 expression, Med. Oncol. 40 (9) (2023) 255.
[23] S. Ashkezari, et al., Antibiotic and inorganic nanoparticles co-loaded into carboxymethyl chitosan-functionalized niosome: synergistic enhanced antibacterial and anti-biofilm activities, J. Drug Deliv. Sci. Technol. 83 (2023), 104386.
[24] F. Hosseini, et al., 3D-printing-assisted synthesis of paclitaxel-loaded niosomes functionalized by cross-linked gelatin/alginate composite: large-scale synthesis and in-vitro anti-cancer evaluation, Int. J. Biol. Macromol. 242 (2023), 124697.
[25] M. Zaer, et al., Doxorubicin-loaded Niosomes functionalized with gelatine and alginate as pH-responsive drug delivery system: a 3D printing approach, Int. J. Biol. Macromol. (2023), 126808.
[26] B. Honarvari, et al., Folate-targeted curcumin-loaded niosomes for site-specific delivery in breast cancer treatment: in silico and in vitro study, Molecules 27 (14) (2022) 4634.
[27] L.E. Kelemen, The role of folate receptor α in cancer development, progression and treatment: cause, consequence or innocent bystander? Int. J. Cancer 119 (2) (2006) 243–250.
[28] D. Jafari-Gharabaghlou, et al., Potentiation of Folate-Functionalized PLGA-PEG nanoparticles loaded with metformin for the treatment of breast Cancer: possible clinical application, Mol. Biol. Rep. 50 (4) (2023) 3023–3033.
[29] S.W. El-Far, et al., Targeting colorectal cancer cells with niosomes systems loaded with two anticancer drugs models; comparative in vitro and anticancer studies, Pharmaceuticals 15 (7) (2022) 816.
[30] T. Rezaei, et al., Folic acid-decorated ph-responsive nanoniosomes with enhanced endocytosis for breast cancer therapy: in vitro studies, Front. Pharmacol. 13 (2022), 851242.
[31] A. Firouzi Amandi, et al., Enhanced anti-cancer effect of artemisinin-and curcumin-loaded niosomal nanoparticles against human colon cancer cells, Med. Oncol. 40 (6) (2023) 170.
[32] E. Salmani-Javan, et al., Fabricating niosomal-PEG nanoparticles co-loaded with metformin and silibinin for effective treatment of human lung cancer cells, Front. Oncol. 13 (2023), 1193708.
[33] A.S. Patil, A.P. Gadad, Development and evaluation of high oxaliplatin loaded CS-g-PNIPAAm co-polymeric nanoparticles for thermo and pH responsive delivery, Indian J. Pharm. Educ. Res 52 (2018) 62–70.
[34] D. Pando, et al., Preparation and characterization of niosomes containing resveratrol, J. Food Eng. 117 (2) (2013) 227–234.
[35] A.P. Tazehkand, et al., The role of Her2-Nrf2 axis in induction of oxaliplatin resistance in colon cancer cells, Biomed. Pharmacother. 103 (2018) 755–766.
[36] P. Ghasemi, et al., Copper nanoparticles induce apoptosis and oxidative stress in Sw480 human colon cancer cell line, Biol. Trace Elem. Res. 201 (8) (2023) 3746–3754.
[37] T. Nayerpour Dizaj, et al., Fabrication of antibody conjugated super magnetic oxide nanoparticles for early detection of prostate cancer, Asian Pac. J. Cancer Prev. APJCP 24 (6) (2023) 2089–2097.
[38] S. Moghassemi, A. Hadjizadeh, Nano-niosomes as nanoscale drug delivery systems: an illustrated review, J. Contr. Release 185 (2014) 22–36.
[39] D. Kaur, S. Kumar, Niosomes: present scenario and future aspects, J. Drug Deliv. Therapeut. 8 (5) (2018) 35–43.
[40] Y. Zhang, et al., Zeta potential: a surface electrical characteristic to probe the interaction of nanoparticles with normal and cancer human breast epithelial cells, Biomed. Microdevices 10 (2008) 321–328.

[41] R. Ridolfo, et al., Exploring the impact of morphology on the properties of biodegradable nanoparticles and their diffusion in complex biological medium, Biomacromolecules 22 (1) (2020) 126–133.
[42] B. Nasseri, Effect of cholesterol and temperature on the elastic properties of niosomal membranes, Int. J. Pharm. 300 (1–2) (2005) 95–101.
[43] R. Shahbazi, et al., Design and optimization various formulations of PEGylated niosomal nanoparticles loaded with phytochemical agents: potential anti-cancer effects against human lung cancer cells, Pharmacol. Rep. 75 (2) (2023) 442–455.